Published in final edited form as:
J Gen Virol. 2012 March ; 93(0 3): 504–515. doi:10.1099/vir.0.038398-0.

Generation and genetic stability of tick-borne encephalitis virus mutants dependent on processing by the foot-and-mouth disease virus 3C protease

Sabrina Schrauf[#1], **Martina Kurz**[#2], **Christian Taucher**[1,‡], **Christian W. Mandl**[1,§], and **Tim Skern**[2]

[1]Institute of Virology, Medical University of Vienna, Kinderspitalgasse 15, A-1095 Vienna, Austria

[2]Max F. Perutz Laboratories, Medical University of Vienna, Dr. Bohr-Gasse 9/3, A-1030 Vienna, Austria

[#] These authors contributed equally to this work.

Abstract

Mature protein C of tick-borne encephalitis virus (TBEV) is cleaved from the polyprotein precursor by the viral NS2B/3 protease (NS2B/3^{pro}). We showed previously that replacement of the NS2B/3^{pro} cleavage site at the C terminus of protein C by the foot-and-mouth disease virus (FMDV) 2A StopGo sequence leads to the production of infectious virions. Here, we show that infectious virions can also be produced from a TBEV mutant bearing an inactivated 2A sequence through the expression of the FMDV 3C protease (3C^{pro}) either *in cis* or *in trans* (from a TBEV replicon). Cleavage at the C terminus of protein C depended on the catalytic activity of 3C^{pro} as well as on the presence of an optimized 3C^{pro} cleavage site. Passage of the TBEV mutants bearing a 3C^{pro} cleavage site either in the absence of 3C^{pro} or in the presence of a catalytically inactive 3C^{pro} led to the appearance of revertants in which protein C cleavage by NS2B/3^{pro} had been regained. In three different revertants, a cleavage site for NS2B/3^{pro}, namely RR*C, was now present, leading to an elongated protein C. Furthermore, two revertants acquired additional mutations in the C terminus of protein C, eliminating two basic residues. Although these latter mutants showed wild-type levels of early RNA synthesis, their foci were smaller and an accumulation of protein C in the cytoplasm was observed. These findings suggest a role of the positive charge of the C terminus of protein C for budding of the nucleocapsid and further support the notion that TBEV protein C is a multifunctional protein.

INTRODUCTION

Tick-borne encephalitis virus (TBEV), from the family *Flaviviridae*, is an enveloped, positive-stranded RNA virus. Its genome is translated into one large polyprotein that traverses the endoplasmic reticulum (ER) several times. This polyprotein is co- and post-translationally cleaved by viral and cellular proteases (Lindenbach *et al.*, 2007). For productive infection, proteolytic processing and assembly of the virus particle must be closely co-ordinated (Amberg & Rice, 1999; Lindenbach *et al.*, 2007). Structural protein processing leads ultimately to the formation of protein C and the two glycoproteins prM (membrane) and E (envelope) (Lobigs, 1993). The latter remain anchored in the ER

Correspondence Tim Skern timothy.skern@meduniwien.ac.at.
[‡]**Present address**: Bristol-Myers Squibb GmbH, Columbusgasse 4, A-1101 Vienna, Austria.
[§]**Present address**: Novartis Vaccines and Diagnostics, Inc., 350 Massachusetts Ave, Cambridge, MA 02139, USA.

Europe PMC Funders Author Manuscripts

membrane, whereas mature protein C participates in RNA packaging and particle assembly with the newly synthesized mRNA to form the nucleocapsid (Mandl, 2005). Preformed nucleocapsid has not yet been detected in infected cells. Given that budding of flavivirus membranes is driven by the interactions of prM and E independently of protein C or the assembled nucleocapsid (Lobigs & Lee, 2004), the co-ordinated cleavage events at the C–prM junction appear to be a key to the efficient incorporation of nucleocapsid during flavivirus assembly.

Cleavage by the viral protease NS2B3 (NS2B/3^{pro}) in the C-terminal region of protein C is a prerequisite for the subsequent signallase cleavage inside the lumen of the ER that generates the N terminus of prM (Amberg & Rice, 1999). The signallase cleavage site of prM is thought to be maintained in a predominantly cryptic conformation until cleavage of C by NS2B/3^{pro}. This prevents cotranslational signallase cleavage of prM and should result in transient expression of a C–prM intermediate at the putative flavivirus assembly site on the ER membrane until cytosolic processing by the viral protease has taken place (Lobigs & Lee, 2004). The importance of the concerted progression of the cleavage events at the C–prM junction has been documented in yellow fever virus, Murray Valley encephalitis virus and TBEV. Inhibition of protein C cleavage or disturbance of the cleavage order interfered with or even abrogated viral growth and infectivity (Amberg & Rice, 1999; Chappell *et al.*, 2005; Lee *et al.*, 2000; Lobigs & Lee, 2004; Schrauf *et al.*, 2008; Stocks & Lobigs, 1998).

The exact position of the TBEV NS2B/3^{pro} protein C cleavage site and the cleavage sequence itself are highly flexible (Schrauf *et al.*, 2008). Furthermore, this NS2B/3^{pro} cleavage site can be replaced by the FMDV (foot-and-mouth disease virus) 2A protein sequence in both TBEV and West Nile Virus (WNV) (Schrauf *et al.*, 2009). This 2A sequence enables the release of mature protein C from the polyprotein in the absence of proteolysis through a ‘StopGo’ mechanism that promotes reinitiation on the translating ribosome (Atkins *et al.*, 2007). The release of protein C thus occurs co-translationally and prematurely compared with that in the wild-type. In addition, the mechanism of action of FMDV 2A results in a protein C with a 19 aa C-terminal extension. Examination of the resulting TBEV mutants showed an altered buoyant density and a reduction of early RNA synthesis upon viral infection but not with electroporation of naked RNA, suggesting previously unrecognized roles of protein C in uncoating and/or early RNA replication (Schrauf *et al.*, 2009).

Here, we further characterize the function(s) of protein C by making the C/prM cleavage dependent on the synthesis of a heterologous protease, the FMDV 3C^{pro} (Curry *et al.*, 2007).

RESULTS

Constructing a system allowing protein C cleavage to be performed by a heterologous protease

TBEV variants in which the NS2B/3^{pro} cleavage site at the C terminus of the protein C had been replaced by the 20 aa FMDV 2A protein still produce infectious virions (Schrauf *et al.*, 2009). Generation of the mature protein C is accomplished by a ‘StopGo’ mechanism in which a PGP motif located at the C-terminal end of the FMDV 2A protein causes the ribosomes to skip peptide bond formation (Donnelly *et al.*, 2001).

Mutants lacking the PGP motif cannot perform the StopGo process, preventing separation of protein C from prM and consequently virion production, even in the presence of viral RNA and protein synthesis. Could the expression of the 3C^{pro} of FMDV rescue mutants lacking PGP by cleaving between the C terminus of protein C and the N terminus the FMDV 2A sequence? To address this question, we took the mutant TBEV 2AΔ3 (Fig. 1a) (Schrauf *et*

al., 2009) lacking the PGP motif at the C terminus of 2A. At the N terminus of the 2A sequence, there is a suboptimal cleavage motif for the FMDV $3C^{pro}$, RGKQ*TLN (the asterisk indicates the cleavage site). To improve this cleavage site, we inserted the amino acids PV and QV between the glycine and lysine residues, optimizing the P4 and P3 positions (Fig. 1a). It has been previously demonstrated (Birtley *et al.*, 2005) that the P4 position is also important for $3C^{pro}$ cleavage. To further enhance the system, we also introduced the mutation E122G into protein E (PV-2AΔ3-H and QV-2AΔ3-H, Fig. 1a). This substitution enables the virus to use heparan sulphate to bind to BHK-21 cells, thus increasing the specific infectivity and binding affinity by up to 10-fold (Kroschewski *et al.*, 2003).

To express FMDV $3C^{pro}$, we used a TBEV replicon lacking the coding region for the structural proteins prM and E (Fig. 1b). This replicon cannot produce infectious viral particles on its own but can replicate RNA and express a heterologous protein from a second ORF at the 3′ end (Gehrke *et al.*, 2005). We placed the FMDV $3C^{pro}$ coding sequence after the EMCV IRES element (ΔME-I-3C, Fig. 1b). We also prepared a replicon expressing an inactive $3C^{pro}$ (ΔME-I-3Ci, Fig. 1b).

The rationale was that when one of the TBEV 2AΔ3 mutants and the protease-encoding TBEV replicon are present within the same cell, the FMDV $3C^{pro}$ expressed from the replicon should recognize its cleavage motif at the C–prM junction of the TBEV-2AΔ3 mutant. This will liberate mature protein C from the signal sequence for prM and allow the signallase to access its cleavage site at the N terminus of prM. These cleavages then enable the generation of all structural proteins leading to the production of single-round infectious particles.

Heterologous expression of the FMDV 3C protease results in virion production

To ensure that replication and protein production still function correctly, we first singly transfected BHK-21 cells with RNAs of ΔME-I-3C, PV-2AΔ3-H and QV-2AΔ3-H. Viral protein expression was analysed after transfection and after the first passage of the supernatant by immunofluorescence (IF) using an antiserum that predominantly recognizes the structural protein E as well as the non-structural protein NS1. Cells transfected with all RNAs showed viral protein expression (Fig. 2a, upper panel). Thus, all RNAs were competent for RNA replication, as we have previously shown that only replication-competent mutants generate and process sufficient proteins to be visible by IF (Kofler *et al.*, 2002). The efficiencies of transfection were approximately 30–40 % for ΔME-I-3C and 80 % for PV-2AΔ3-H and QV-2AΔ3H (Fig. 2a, upper panel). As the replicons do not express protein E, it is possible that the efficiency of their transfection is underestimated compared with those of the modified viruses that express both protein E and NS1 that can be recognized by the antiserum used. Twenty-four hours later, phase-contrast microscopy revealed that cells transfected with these showed a strong cytopathic effect (CPE) with the concomitant death of the majority of cells. Passaging of supernatants from the transfected cells did not, however, lead to the production of viable virus (Fig. 2a, lower panel).

We then transfected PV-2AΔ3-H or QV-2AΔ3-H RNAs together with RNA from the replicon ΔME-I-3C. After 24 h, cells stained almost 100% positive for viral protein expression (Fig. 2b, upper panel), indicating a high electroporation efficiency. As the two replicating constructs both produce the NS1 protein, the antiserum (predominantly recognizing proteins E and NS1) cannot distinguish between them; therefore, we were not able to determine how many cells were double-positive. Nevertheless, IF analysis of singly transfected cells (80–90% for the TBEV-mutant RNAs and 30–40% for the ΔME-I-3C replicon RNA) indicated that at least 20–30% of the co-transfected cells expressed both constructs. We then used the supernatants of the electroporated cells to infect fresh BHK

cells. Using supernatants transfected with the RNAs PV-2AΔ3-H and ΔME-I-3C, about 40–50% of the fresh BHK cells were positive for the production of viral proteins as detected by IF using the antiserum staining for the proteins E and NS1, indicating that virions had been produced by doubly transfected cells (Fig. 2b, lower panel). In contrast, no positive cells were observed with supernatants from cells transfected with QV-2AΔ3-H or ΔME-I-3C RNA (Fig. 2b), suggesting that the only cleavage site recognized was that with the optimal PV sequence at P3 and P4.

Virion production depends on expression of an active 3C protease

The above results implied that the FMDV $3C^{pro}$ could rescue the defect in PV-2AΔ3-H. To provide further evidence and to exclude any involvement of NS2B/3^{pro}, we constructed a ΔME replicon containing an inactive $3C^{pro}$ (ΔME-I-3Ci; Fig. 1b) in which the active site cysteine (Cys163) had been mutated to alanine. Cells transfected with ΔME-I-3Ci RNA alone showed viral protein expression and a CPE (Fig. 2a and data not shown). However, the supernatant of cells co-transfected with ΔME-I-3Ci and PV-2AΔ3-H RNAs did not contain any infectious particles (Fig. 2b). This strengthens the notion that an active $3C^{pro}$ is required for virion production from PV-2AΔ3-H and that the $3C^{pro}$ can replace the NS2B/3^{pro} in protein C cleavage.

Protein prM is only formed in the presence of an active 3C protease

To assess protein processing at the C–prM junction in cells transfected with full-length TBEV mutants and the ΔME replicons, we examined protein prM production. All constructs used [i.e. the full-length TBEV mutants (Fig. 1a) and the ΔME replicon (Fig. 1b)] code for protein C; therefore, its analysis provides no information on $3C^{pro}$ cleavage. However, protein prM is only expressed in cells containing the TBEV mutants when $3C^{pro}$ cleaves at the cytoplasmic side of the signal sequence for prM, allowing the signallase access to its cleavage site at the N terminus of protein prM. We therefore lysed cells transfected with various RNAs 22 h after transfection and detected the structural proteins E and prM with polyclonal antisera raised against all structural proteins of TBEV and against prM itself, respectively (Fig. 3). A prominent band corresponding to protein E, indicating viral protein synthesis and processing, was detected in lysates of cells transfected with a full-length TBEV mutant (Fig. 3, upper panel). In contrast, the band was absent from the lysate transfected with the ΔME replicon alone. With the anti-prM serum (Fig. 3, lower panel), a prominent band with a size corresponding to that of protein prM was only detected in lysates of cells transfected with combinations of PV-2AΔ3-H+ΔME-I-3C or PV-2AΔ3+ΔME-I-3C (Fig. 3, lower panel, lanes 4 and 7). Cell lysates of the full-length TBEV mutants with the PV-2AΔ3 motif either alone or in combination with ΔME-I-3Ci failed to produce any protein prM, indicating no protein processing at the C–prM junction in the absence of an active $3C^{pro}$. Furthermore, no protein prM was visible in lysates from cells transfected with RNAs containing the QV-Δ3-H motif alone or in combination with the $3C^{pro}$, indicating that the $3C^{pro}$ cleavage requires a suitable P4 residue. We did not, however, observe any uncleaved C-2AΔ3-prM protein in the Western blot with the anti-prM antiserum (Fig. 3, lower panel). We believe that this is due to the high background at the predicted position (about 35 kDa) as well as a previously observed inability of this antiserum to recognize the C–prM protein. No differences were visible between lysates containing the PV-2AΔ3 mutant with or without the heparan sulphate mutation; hence, this additional mutation has no impact on processing of the structural proteins (Fig. 3, lanes 4 and 7).

Supplying the 3C protease *in cis* also results in TBEV mutant virion production

Can $3C^{pro}$ also be provided *in cis*? Accordingly, we constructed full-length TBEV mutants containing the $3C^{pro}$ cleavage motif P-V-K-Q*T at the C terminus of protein C as well as

the coding region for an active or inactive $3C^{pro}$ as a second cistron under IRES control (Fig. 4a). The protein E heparan sulphate mutation was present in all constructs.

RNAs of PV-2AΔ3-H-I-3C and PV-2AΔ3-H-I-3Ci were transfected into BHK-21 cells and viral protein expression was examined by IF analysis (Fig. 4b, upper panel). About 30–40% of cells transfected with both mutants exhibited a positive IF staining, indicating that both mutants were competent for replication and protein expression. Next, supernatants of the transfected cells were applied to fresh cells and infection of these cells was again monitored by IF (Fig. 4b, lower panel). RNA from PV-2AΔ3-H-I-3C produced infectious virions and could be propagated further as indicated by the detection of positive cells after the first passage. No infectious virions were obtained with PV-2AΔ3-H-I-3Ci containing an inactive $3C^{pro}$.

Thus, the presence of the $3C^{pro}$ cleavage site and the $3C^{pro}$ sequence on the same genome also allows virion production. However, the efficiency was lower than when $3C^{pro}$ was supplied *in trans*.

Passage of 3C protein C cleavage site mutants in the absence of an active 3C protease provokes resuscitating mutations

Now, we wished to examine how quickly mutants could arise in the absence of an active $3C^{pro}$ that would allow the formation of a new NS2B/3^{pro} protein C cleavage site and thus lead to the production of infectious virions. Accordingly, passaging experiments on BHK-21 cells were performed. First, *in vitro*-synthesized RNAs of PV-2AΔ3-H, QV-2AΔ3-H, PV-2AΔ3-H-I-3Ci as well as PV-2AΔ3-H together with RNA of the replicon ΔME-I-3Ci were electroporated into BHK-21 cells. Then, supernatants from the transfected cells were harvested 1 or 2 days post-transfection and transferred onto fresh BHK-21 cells; infection of cells was determined by IF. Cells inoculated with supernatants from day 1 were all negative for viral protein expression (Fig. 5a). Surprisingly, however, in one of three attempts, 100% of the cells inoculated with 2 day supernatants derived from PV-2AΔ3-H transfected cells and about 50% of cells inoculated with those from QV-2A3Δ-H and PV-2AΔ3-H-I-3Ci exhibited a bright IF staining (Fig. 5a), indicating the production of infectious virions. In contrast, no positive IF was observed with supernatants from cells transfected with the two RNAs PV-2AΔ3-H+ΔME-I-3Ci (data not shown).

To identify the responsible mutations, viral RNA was isolated from supernatants 3 days post-infection of the second passage and the entire structural protein-coding region (C–prM–E), as well as the domain comprising the heterologous inactive 3C protease was sequenced. No mutations were found within the protease domain; however, all three mutants had acquired a one nucleotide insertion and a one nucleotide deletion in the structural protein coding region that led to a short change of the reading frame. In PV-2AΔ3-H, 6 aa within the 2AΔ3 protein sequence were provided from another reading frame (Fig. 5b). In contrast, QV-2AΔ3-H and PV-2AΔ3-H-I-3Ci, 22 aa in the C-terminal region of protein C and the 2AΔ3 protein sequence were provided from the same reading frame as in PV-2AΔ3-H (Fig. 5b). These alterations not only changed 2AΔ3 hydrophobicity but also introduced a potential NS2B/3^{pro} cleavage motif of R-R*C at identical locations in all three revertants.

To ensure that these frame-shifts were responsible for the restoration of infectivity, we introduced the mutations observed in Fig. 5 into the full-length TBEV-2AΔ3 clone and transfected the RNAs PV-2AΔ3-mut1, PV-2AΔ3-mut2 and QV-2AΔ3-mut into BHK-21 cells. Infectious virions were indeed obtained after passage of the transfection supernatants (data not shown). These passaging experiments also revealed that the virions of PV-2AΔ3-mut2 and QV-2AΔ3-mut had a lower infectivity than PV-2AΔ3-mut1, possibly due to the changes in protein C.

Was the sequence R-R*C being recognized by the TBEV NS2B/3^{pro}? Accordingly, we transfected BHK-21 cells with WT-TBEV and mutant RNAs and lysed cells 48 h post-transfection. As expected, WT-TBEV lysates showed prominent bands for the structural proteins E, prM and C (Fig. 6, lane 2), whereas the mutants showed only prM and E but no C band. Instead a new band was visible, termed C* (Fig. 6, lane 3, 4 and 5), running slightly slower than the wild-type. The size would correspond to a protein C extended by 14 aa, further indicating that the R-R*C motif is processed by the NS2B/3^{pro}. Moreover, the ratio of intracellular protein C to the surface proteins prM and E differed in the mutants. Thus, PV-2AΔ3-mut1 has a C/E ratio similar to that of the WT-TBEV, whereas PV-2AΔ3-mut2 and QV-2AΔ3-mut (Fig. 6, lane 4 and 5) show a much higher ratio, suggesting that protein C accumulates in the cytoplasm.

QV-2AΔ3-mut1 and PV-2AΔ3-mut are impaired in viral spread

To determine differences in infectious virus progeny production, we examined the ability of the revertants to form foci. WT-TBEV was used as a positive control. As a further control, TBEV-2A was included into the experiments, as its protein C comprises four amino acids more than the second-site revertants and has already been characterized. TBEV-2A foci are 10 times smaller than those produced by the WT-TBEV, and can only be visualized 70 h post-infection, clearly indicating a defect in viral spread (Schrauf *et al.*, 2009). Interestingly, despite the 14 aa extension of its protein C, foci formed by PV-2AΔ3-mut1 were only marginally smaller than those formed by the WT-TBEV and could be detected 50 h post-infection (Fig. 7a, bottom). In contrast, PV-2AΔ3-mut2 and QV-2A3Δ-mut formed foci that could be visualized only 70 h post-infection and were considerably smaller than those of the WT-TBEV. However, they were still about three to four times larger than those of TBEV-2A (Fig. 7a, top).

To quantify the observed differences in infectivity, we compared the growth properties of WT-TBEV, TBEV-2A and the three second site mutants. We performed multistep growth curves in BHK-21 cells at a low m.o.i. of 0.01 as shown in Fig. 7(b). As previously observed (Schrauf *et al.*, 2009), TBEV-2A showed a delayed and reduced particle release. In contrast, PV-2AΔ3-mut1, which forms large foci, produced infectious progeny close to WT level, whereas QV-2AΔ3-mut1 and PV-2AΔ3-mut2 showed infectivity titres 1 and 1.5 log units below those of the WT but still between 2.5 and 1.5 log units higher than TBEV-2A (Fig. 7b).

PV-2AΔ3-mut1 exhibits a delay in the onset of early RNA replication

The observed defects in infectivity and viral spread of TBEV-2A were proposed to result from an impairment of unpackaging and early RNA synthesis (Schrauf *et al.*, 2009). To determine the effect of protein C extensions of the revertants on viral replication, we examined early RNA synthesis after infection. As expected, TBEV-2A exhibited a delayed and reduced RNA replication (Fig. 8). Interestingly, mutant PV-2AΔ3-mut1 also showed a delay in the onset of RNA replication during the first 6 h post-infection. Nevertheless, after the onset of RNA replication, no further impairment in RNA synthesis was detectable. Indeed, already 9 h post-infection, this mutant produced as many RNA molecules as the WT-TBEV, which is in good accordance with the results shown in Fig. 7. In contrast, PV-2AΔ3-mut2 and QV-2AΔ3-mut produced similar amounts of RNA copies (Fig. 8). Thus, the reduction of foci size and infectivity of PV-2AΔ3-mut2 and QV-2AΔ3-mut does not appear to be the result of an impaired RNA replication.

DISCUSSION

We show here that the production of infectious flaviviral virions can be dependent on protein C cleavage by a heterologous protease, the FMDV $3C^{pro}$. Virion production was enabled by providing the enzyme either *in cis* or *in trans* from a TBEV replicon. Virion assembly was more efficient when the 3C protease was provided *in trans*. Most probably, in the *cis* construction, protein synthesis from the 5′ end of the TBEV genome was lowered by the presence of the IRES element in the 3′ non-coding region. This has also been observed in bicistronic TBEV mutants in which an IRES element controls the expression of the structural proteins prM and E (Orlinger *et al.*, 2006).

Cell-based antiviral assays in which the production of infectious virions depends on cleavage by HCV NS3 protease have been reported (Filocamo *et al.*, 1997; Hahm *et al.*, 1996; Lai *et al.*, 2000). Our system is, however, the first to enable the recovery of a non-infectious virus through a second replicon expressing the required protease. To assess the genetic stability of this system, we investigated how rapidly monocistronic full-length TBEV mutants PV-2AΔ3-H and QV-2AΔ3-H would acquire spontaneous mutations during passage on BHK-21 cells in the absence of the $3C^{pro}$. Similarly, we also investigated the bicistronic PV-2AΔ3-H-I-3Ci construction that contains an inactive $3C^{pro}$ as well as the monocistronic full-length TBEV mutant PV-2AΔ3-H together with the TBEV replicon expressing an inactive $3C^{pro}$. Multiple amino acid changes at the C–prM junction were observed in the PV-2AΔ3-H and QV-2AΔ3-H mutants as well as in PV-2AΔ3-H-I-3Ci but not in the PV-2AΔ3-H transfected with the TBEV replicon expressing the inactive $3C^{pro}$. This indicates that the *trans*-complementation system is more stable than the *cis* system.

The specific changes in the revertants all resulted from the insertion of one nucleotide and the deletion of a second. Throughout, an NS2B/3^{pro} cleavage motif R-R*C was introduced at an identical location in the 2AΔ3 region so that cleavage at this sequence by NS2B/3^{pro} should give rise to a C-terminal extension of 14 aa in protein C in all three revertants. Furthermore, in PV-2AΔ3-H, six amino acids within the 2AΔ3 protein sequence were mutated, whereas in QV-2AΔ3-H and PV-2AΔ3-H-3Ci, the insertion and deletion led to the mutation of the same 22 aa, located in both the C-terminal region of protein C and the 2AΔ3 protein sequence. The new amino acid sequences differed only in the most C-terminal amino acid of the mutated region (Fig. 5b).

Introduction of the mutations into TBEV-2AΔ3 confirmed that they restored the production of infectious virus progeny. In addition, protein C of all three mutants showed a slower mobility on SDS-PAGE than the WT (Fig. 6), strongly suggesting that cleavage was performed by NS2B/3^{pro} at the putative cleavage site.

Differences in the properties of the revertants were evident. PV-2AΔ3-H-mut1 reached wild-type levels both in infectivity and RNA synthesis and showed only a minor effect on viral spread. However, a delay in the onset of early RNA replication was detectable. The other mutants PV-2AΔ3-H-mut2 and QV-2AΔ3-H-mut that bear the almost identical 22 aa change also grew to high titres, just 1 and 1.5 log units lower than WT-TBEV, respectively. Both exhibited a smaller foci size, even though their RNA replication was similar to the WT-TBEV level.

The origin of these differences might be the more hydrophilic character of the protein C extension of all three revertants (compared with that of TBEV-2A), which would favour both the infectivity and early RNA synthesis. This agrees with our previous work on TBEV-2A, indicating that a hydrophobic extension to protein C can interfere with particle formation, viral spread and early RNA replication (Schrauf *et al.*, 2009). The different

behaviour of the revertants in the onset of early RNA replication described here can be also attributed to the composition of the protein C extension. A comparison of all three revertants and TBEV-2A reveals that the more hydrophobic the extension of protein C, the lower the rate of early RNA synthesis in general and the later the onset of early RNA replication and/or unpackaging in particular.

The amino acid changes of mutants PV-2AΔ3-H-mut2 and QV-2AΔ3-H-mut resulted in a more hydrophilic 2AΔ3 region than in the case of PV-2AΔ3-H-mut1. Consequently, these two mutants have no impairment in the onset of early RNA synthesis, in marked contrast to the 6 h delay of PV-2AΔ3-H-mut1. TBEV-2A, however, which possesses an extension of mainly hydrophobic amino acids showed both a delay as well as a reduction in early RNA synthesis. Finally, the observed difference between the revertants and TBEV-2A also suggests that the re-establishment of a NS2B/3^{pro} cleavage in the C-terminal region of C is advantageous for viral spread.

Despite these beneficial contributions, the more hydrophilic character of the extension did not aid viral spread. PV-2AΔ3-H-mut2 and QV-2AΔ3-H-mut, which carry more hydrophilic amino acids in the 2AΔ3 region than PV-2AΔ3-H-mut1, formed considerably smaller foci that could be visualized only 3 days post-infection. In contrast, the foci of PV-2AΔ3-H-mut1 were only marginally smaller than those of the WT. The difference appears to lie in the C-terminal part of protein C, where only PV-2AΔ3-H-mut2 and QV-2AΔ3-H-mut have acquired additional mutations. These mutations led to the loss of two basic amino acids in the C-terminal part of protein C. Ma, Dokland and their co-workers (Dokland *et al.*, 2004; Ma *et al.*, 2004) have shown for dengue virus and WNV protein C that protein C occurs as a dimer with the two C-terminal helices forming a broad interface for interaction with RNA. Therefore, the loss of positive charges close to the helix may hinder correct dimer formation and/or RNA binding. Given that the RNA production upon infection was at wild-type levels (Fig. 8), we can exclude a defect in unpackaging or synthesis of RNA. In contrast, we propose that the accumulation of protein C in the cytoplasm is crucial (Fig. 6), indicating that the reduced infectivity of PV-2AΔ3-H-mut2 or QV-2AΔ3-H-mut is caused by a defect in formation and/or budding of the NC, thus limiting viral spread. In contrast, the protein C of the PV-2AΔ3-H-mut1 was not affected by the amino acid changes and no accumulation of protein C in the cytoplasm occurred (Fig. 6), indicating that budding was undisturbed. Our results highlight therefore a previously undetected role of the C terminus of protein C for budding of the NC and the necessity of positive charges.

METHODS

Plasmids and cells

All TBEV constructs derive from the cDNA of TBEV strain Neudoerfl (GenBank accession no. U27495) (Mandl *et al.*, 1997). BHK-21 (ATCC CCL10) cells were cultured as described previously (Schrauf *et al.*, 2008). Oligonucleotides are listed in Supplementary Table S1.

Full-length TBEV mutants

pTNd/5′ (Schrauf *et al.*, 2008) and all derivatives of pTNd/5′ contain the 5′ one-third of the cDNA of TBEV strain Neudoerfl genome. Infectious full-length RNA was generated after *in vitro* ligation of the 5′ cDNA clones with the 3′ cDNA clone pTNd/3′ (Schrauf *et al.*, 2008), which contains the 3′ two-thirds of the TBEV genome. Plasmid p2AΔ3/5′ was constructed by deleting the PGP motif at the C-terminal end of the FMDV-2A protein sequence of TBEV-2A/5′. For plasmid pPV-2AΔ3/5′, the P4 (proline) and the P3 positions (valine) of the 3C^{pro} cleavage site were introduced upstream of lysine 94 of the TBEV protein C using the forward primer P43-F, the reverse primer P43-R and p2A3Δ/5′ as template. Plasmid

pPV-2A3Δ-H/5′, containing the P4 and P3 positions of the $3C^{pro}$ cleavage site as well as the heparan sulphate mutation E122G in protein E, was generated using the forward primer E122G-F, the reverse primer E122G-R and pPV-2A3Δ/5′ as template. Plasmid pQV-2A3Δ-H/5′, containing valine instead of proline at the P4 position of the $3C^{pro}$ cleavage site, was created using the forward primer PQ-F, the reverse primer PQ-R and pPV-2A3Δ-H/5′ as template.

Plasmid pTNd/c contains a full-length genomic cDNA of the WT TBEV strain Neudoerfl. TBEV-2A contains a functional FMDV-2A sequence that replaces the NS2B/3 cleavage site between protein C and prM. RNA of TBEV mutants with resuscitating mutations in the 2AΔ3 region was isolated, reverse transcribed and cloned into the pTNd/c cDNA using restriction sites for *Sal*I and *Sna*BI; the cDNAs have no heparan sulphate mutation.

TBEV replicons

Replicons ΔME-I-3C and ΔME-I-3Ci are derivatives of clone ΔME–eGFP (Gehrke *et al.*, 2005), expressing the eGFP under the control of the ECMV IRES. The replicon ΔME-I-3C was created by a three-step PCR strategy. PCR-I was performed using the forward primer *Avr*II-F, the reverse primer IRES-3C-R and plasmid ME–ΔeGFP as template. PCR-II amplified the $3C^{pro}$ with the forward primer IRES-3C-F, the reverse primer 3C-*Age*I-R and plasmid pET-3C (provided by Francois Maree, Onderstepoort, South Africa, containing the FMDV 3C sequence of strain O/SAR/19/00) as template. PCR-III was then performed with primers *AvrII*-F and 3C-*Age*I-R using PCR products I and II as template. Then, the *Avr*II–*Age*I fragment of ΔME–eGFP was replaced by the *Avr*II and *Age*I restricted PCR product III to generate ΔME-I-3C. Replicon ΔME-I-3Ci, containing a cysteine-to-alanine mutation at position 163 of the 3C protease, was constructed in a similar way as described above, with the primer combinations *Avr*II-F and C163A-R for PCR-I and C163A-F and *Age*I-R for PCR-II. As template, ΔME-I-3C was used.

Plasmid ΔME-I-3C was amplified in *Escherichia coli* Copy Cutter EPI400 (Epicentre) *E. coli* HB101 was used for all other plasmids.

RNA transcription and transfection

Transcription of RNA *in vitro* and transfection into BHK-21 cells by electroporation were as described previously (Mandl *et al.*, 1997; Schrauf *et al.*, 2008).

Detection of viral proteins

Viral protein expression was examined by IF staining and Western blotting. For IF, transfected BHK-21 cells were disseminated into 24-well tissue culture plates containing microscope coverslips and permeabilized by acetone-methanol fixation (1 : 1) 1 day post-transfection. Expression of the structural proteins C, prM and E and the non-structural protein NS1 was visualized by successive incubation with a rabbit polyclonal anti-TBEV serum predominantly recognizing protein E and protein NS1 and fluorescein-isothiocyanate-conjugated anti-rabbit antibody (Jackson Immune Research Laboratory). For passaging experiments, supernatants from transfected BHK-21 cells seeded in 25 cm^2 tissue culture flasks were transferred onto fresh BHK-21 cells 1 day post-transfection and viral protein expression was analysed as described above 1 day post-infection. For the selection of resuscitating mutations, supernatants from transfected cell cultures were applied to fresh cells 2 days post-electroporation and, after a second round of passage, viral protein expression determined.

Formation of the structural proteins prM and E was monitored by immunoblotting (Schrauf *et al.*, 2008).

Virus stock preparation

To generate virus stocks, BHK-21 cells were electroporated with RNAs of WT-TBEV, TBEV-2A, PV-2AΔ3-mut1, PV-2AΔ3-mut2 and QV-2AΔ3-mut, respectively. Supernatants were harvested 48 h post-electroporation. RNA was isolated from these stocks, followed by reverse transcription. Constructs were confirmed by sequencing. Titre and focus morphology were determined by focus assay.

Multistep growth curves

BHK-21 monolayers grown in six-well plates were infected with stock preparations of respective viruses at a m.o.i of 0.01. Aliquots of supernatants were collected at various time points and infectious particles were quantified by focus assay.

Focus assay

To quantify the production of infectious virus particles, an immunochemical focus assay was employed (Schrauf *et al.*, 2009).

RNA replication

Intracellular RNA replication after infection was determined as described previously (Schrauf *et al.*, 2009).

Protein sequence analysis

Hydrophobicity plots were done using the DNASTAR programme PROTEAN (Kyle-doolitle scale, window size 11).

Supplementary Material

Refer to Web version on PubMed Central for supplementary material.

Acknowledgments

We thank Francois Maree for providing the FMDV 3C sequence. This project was funded by the Austrian Science fund, grant FWF-P19528 to T. S.

REFERENCES

Amberg SM, Rice CM. Mutagenesis of the NS2B-NS3-mediated cleavage site in the flavivirus capsid protein demonstrates a requirement for coordinated processing. J Virol. 1999; 73:8083–8094. [PubMed: 10482557]

Atkins JF, Wills NM, Loughran G, Wu CY, Parsawar K, Ryan MD, Wang CH, Nelson CC. A case for “StopGo”: reprogramming translation to augment codon meaning of GGN by promoting unconventional termination (Stop) after addition of glycine and then allowing continued translation (Go). RNA. 2007; 13:803–810. [PubMed: 17456564]

Birtley JR, Knox SR, Jaulent AM, Brick P, Leatherbarrow RJ, Curry S. Crystal structure of foot-and-mouth disease virus 3C protease. New insights into catalytic mechanism and cleavage specificity. J Biol Chem. 2005; 280:11520–11527. [PubMed: 15654079]

Chappell KJ, Nall TA, Stoermer MJ, Fang NX, Tyndall JD, Fairlie DP, Young PR. Site-directed mutagenesis and kinetic studies of the West Nile Virus NS3 protease identify key enzyme-substrate interactions. J Biol Chem. 2005; 280:2896–2903. [PubMed: 15494419]

Curry S, Roqué-Rosell N, Zunszain PA, Leatherbarrow RJ. Foot-and-mouth disease virus 3C protease: recent structural and functional insights into an antiviral target. Int J Biochem Cell Biol. 2007; 39:1–6. [PubMed: 16979372]

Dokland T, Walsh M, Mackenzie JM, Khromykh AA, Ee KH, Wang S. West Nile virus core protein; tetramer structure and ribbon formation. Structure. 2004; 12:1157–1163. [PubMed: 15242592]

Donnelly ML, Luke G, Mehrotra A, Li X, Hughes LE, Gani D, Ryan MD. Analysis of the aphthovirus 2A/2B polyprotein 'cleavage' mechanism indicates not a proteolytic reaction, but a novel translational effect: a putative ribosomal 'skip'. J Gen Virol. 2001; 82:1013–1025. [PubMed: 11297676]

Filocamo G, Pacini L, Migliaccio G. Chimeric Sindbis viruses dependent on the NS3 protease of hepatitis C virus. J Virol. 1997; 71:1417–1427. [PubMed: 8995667]

Gehrke R, Heinz FX, Davis NL, Mandl CW. Heterologous gene expression by infectious and replicon vectors derived from tick-borne encephalitis virus and direct comparison of this flavivirus system with an alphavirus replicon. J Gen Virol. 2005; 86:1045–1053. [PubMed: 15784898]

Hahm B, Back SH, Lee TG, Wimmer E, Jang SK. Generation of a novel poliovirus with a requirement of hepatitis C virus protease NS3 activity. Virology. 1996; 226:318–326. [PubMed: 8955051]

Kofler RM, Heinz FX, Mandl CW. Capsid protein C of tick-borne encephalitis virus tolerates large internal deletions and is a favorable target for attenuation of virulence. J Virol. 2002; 76:3534–3543. [PubMed: 11884577]

Kroschewski H, Allison SL, Heinz FX, Mandl CW. Role of heparan sulfate for attachment and entry of tick-borne encephalitis virus. Virology. 2003; 308:92–100. [PubMed: 12706093]

Lai VC, Zhong W, Skelton A, Ingravallo P, Vassilev V, Donis RO, Hong Z, Lau JY. Generation and characterization of a hepatitis C virus NS3 protease-dependent bovine viral diarrhea virus. J Virol. 2000; 74:6339–6347. [PubMed: 10864644]

Lee E, Stocks CE, Amberg SM, Rice CM, Lobigs M. Mutagenesis of the signal sequence of yellow fever virus prM protein: enhancement of signalase cleavage In vitro is lethal for virus production. J Virol. 2000; 74:24–32. [PubMed: 10590087]

Lindenbach, BD.; Thiel, HJ.; Rice, CM. Flaviviridae: the viruses and their replication. In: Knipe, DM.; Howley, PM., editors. Fields Virology. Lippincott Williams & Wilkins; Philadelphia: 2007. p. 1101-1152.

Lobigs M. Flavivirus premembrane protein cleavage and spike heterodimer secretion require the function of the viral proteinase NS3. Proc Natl Acad Sci U S A. 1993; 90:6218–6222. [PubMed: 8392191]

Lobigs M, Lee E. Inefficient signalase cleavage promotes efficient nucleocapsid incorporation into budding flavivirus membranes. J Virol. 2004; 78:178–186. [PubMed: 14671099]

Ma L, Jones CT, Groesch TD, Kuhn RJ, Post CB. Solution structure of dengue virus capsid protein reveals another fold. Proc Natl Acad Sci U S A. 2004; 101:3414–3419. [PubMed: 14993605]

Mandl CW. Steps of the tick-borne encephalitis virus replication cycle that affect neuropathogenesis. Virus Res. 2005; 111:161–174. [PubMed: 15871909]

Mandl CW, Ecker M, Holzmann H, Kunz C, Heinz FX. Infectious cDNA clones of tick-borne encephalitis virus European subtype prototypic strain Neudoerfl and high virulence strain Hypr. J Gen Virol. 1997; 78:1049–1057. [PubMed: 9152422]

Orlinger KK, Hoenninger VM, Kofler RM, Mandl CW. Construction and mutagenesis of an artificial bicistronic tick-borne encephalitis virus genome reveals an essential function of the second transmembrane region of protein e in flavivirus assembly. J Virol. 2006; 80:12197–12208. [PubMed: 17035331]

Schrauf S, Schlick P, Skern T, Mandl CW. Functional analysis of potential carboxy-terminal cleavage sites of tick-borne encephalitis virus capsid protein. J Virol. 2008; 82:2218–2229. [PubMed: 18160443]

Schrauf S, Mandl CW, Bell-Sakyi L, Skern T. Extension of flavivirus protein C differentially affects early RNA synthesis and growth in mammalian and arthropod host cells. J Virol. 2009; 83:11201–11210. [PubMed: 19692461]

Stocks CE, Lobigs M. Signal peptidase cleavage at the flavivirus C-prM junction: dependence on the viral NS2B-3 protease for efficient processing requires determinants in C, the signal peptide, and prM. J Virol. 1998; 72:2141–2149. [PubMed: 9499070]

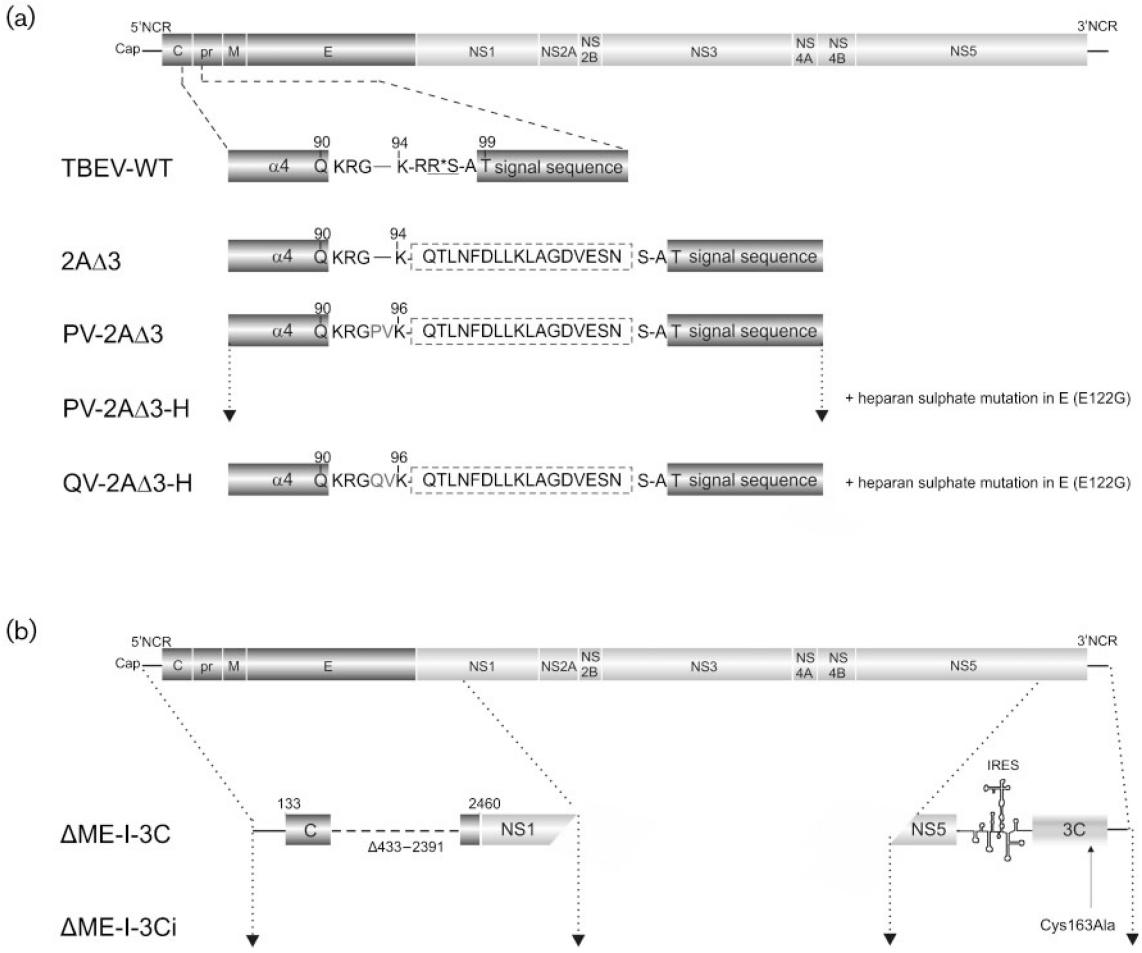

Fig. 1.

Structural organization of flavivirus mutants. (a) Drawing of the TBEV full-length genome and expanded views of the protein C of TBEV WT and each TBEV mutant (not drawn to scale). The NS2B/3 cleavage site is underlined and the cleavage position is marked by an asterisk. The inserted FMDV 2AΔ3 protein sequence is surrounded by a dashed line. The amino acids PV and QV preceding residue K96 were inserted to optimize the FMDV $3C^{pro}$ cleavage sequence. The numbers at the top refer to the amino acid positions within protein C. (b) Diagram of the TBEV genome and an expanded view of the structural protein region and the 3′NCR of each constructed TBEV replicon. The $3C^{pro}$ sequence was amplified by PCR from the FMDV strain O/SAR/19/00 and placed behind an EMCV IRES as described in methods. Engineered mutations are shown with the corresponding designation.

Europe PMC Funders Author Manuscripts

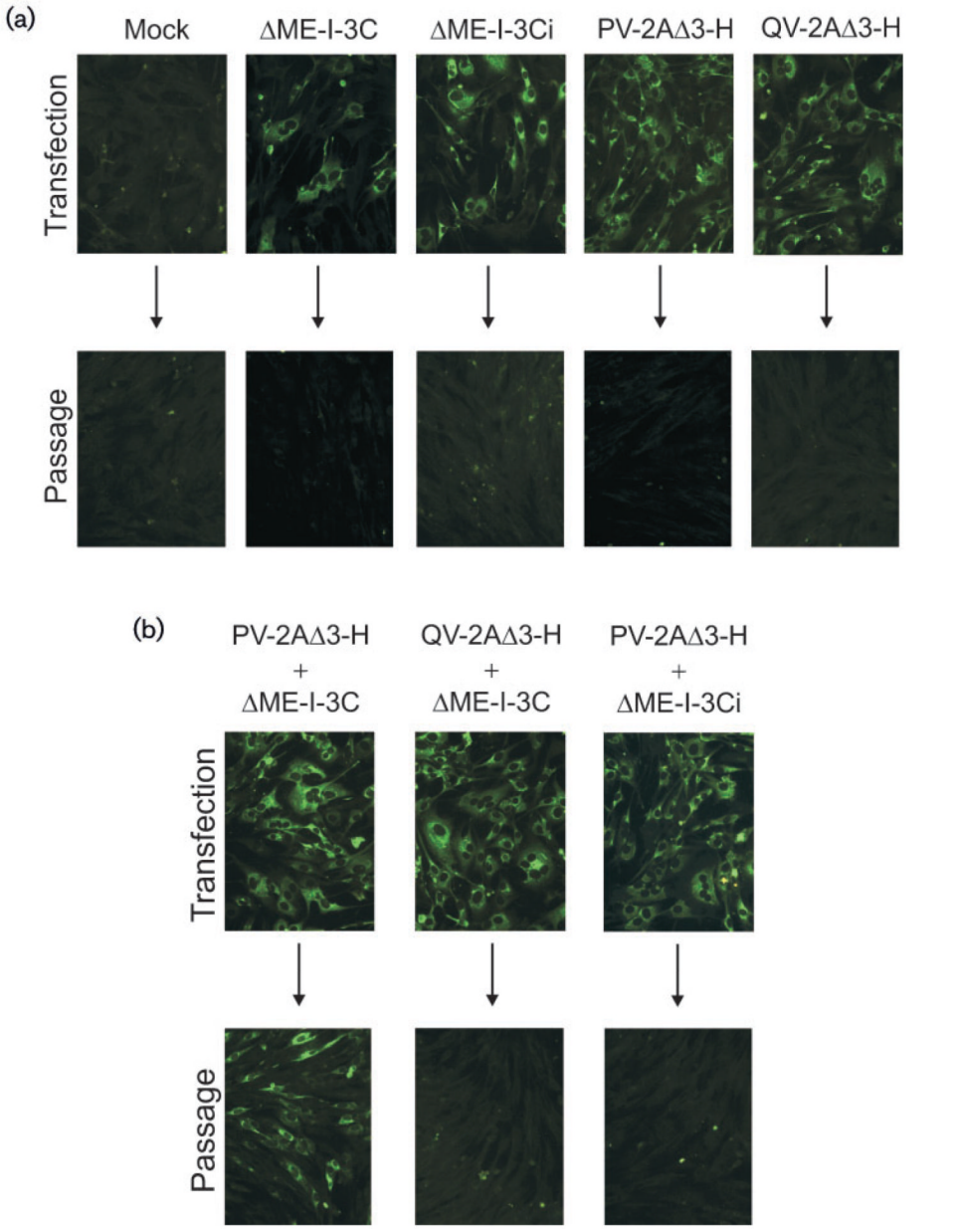

Fig. 2.

Cotransfection of TBEV PV-2AΔ3-H and QV-2AΔ3H with TBEV replicons expressing active or inactive $3C^{pro}$. (a and b) BHK-21 cells were transfected with mutant RNAs or were mock transfected and viral protein expression was detected with a polyclonal serum 1 day post-transfection. Supernatants harvested 1 day post-electroporation were used to inoculate fresh BHK-21 cells (arrows), and viral protein expression monitored by IF 1 day post-infection (bottom of panels a and b).

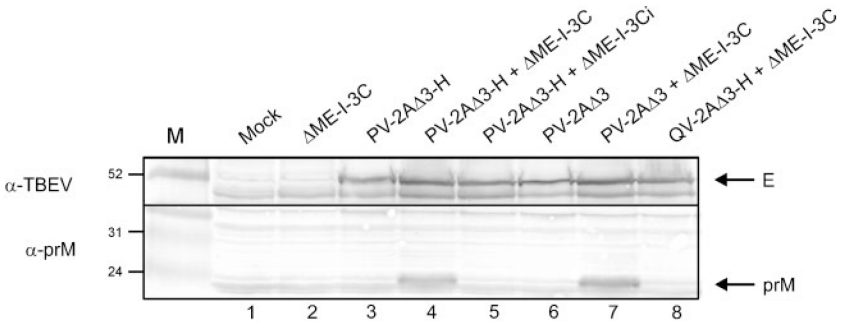

Fig. 3.

Western blot analysis of structural protein processing. Cells transfected with mutant RNAs were lysed 22 h post-transfection, and structural proteins prM and E were detected using polyclonal sera. Positions of marker proteins in kDa are marked

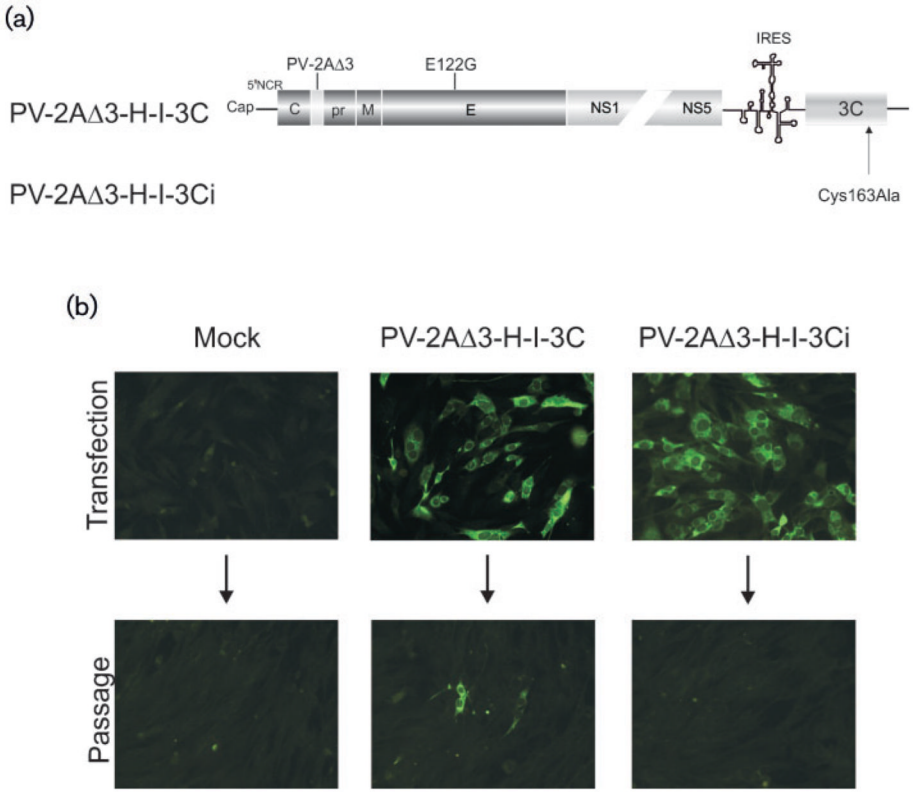

Fig. 4.

Analysis of TBEV mutants expressing the $3C^{pro}$ cleavage site and the $3C^{pro}$ on the same construct. (a) Schematic of TBEV full-length mutants with the PV-2AΔ3 insertion within the C-terminal region of protein C, the heparan sulphate mutation in E and the $3C^{pro}$. (b) IF analysis of viral protein expression and viral infectivity. BHK-21 cells were transfected with mutant RNAs or were mock transfected, and viral protein expression was detected by IF with the polyclonal serum 1 day post-transfection (top). Supernatants harvested 1 day post-electroporation were also transferred onto fresh BHK-21 cells (arrows), and viral protein expression monitored by IF 1 day post-infection (bottom).

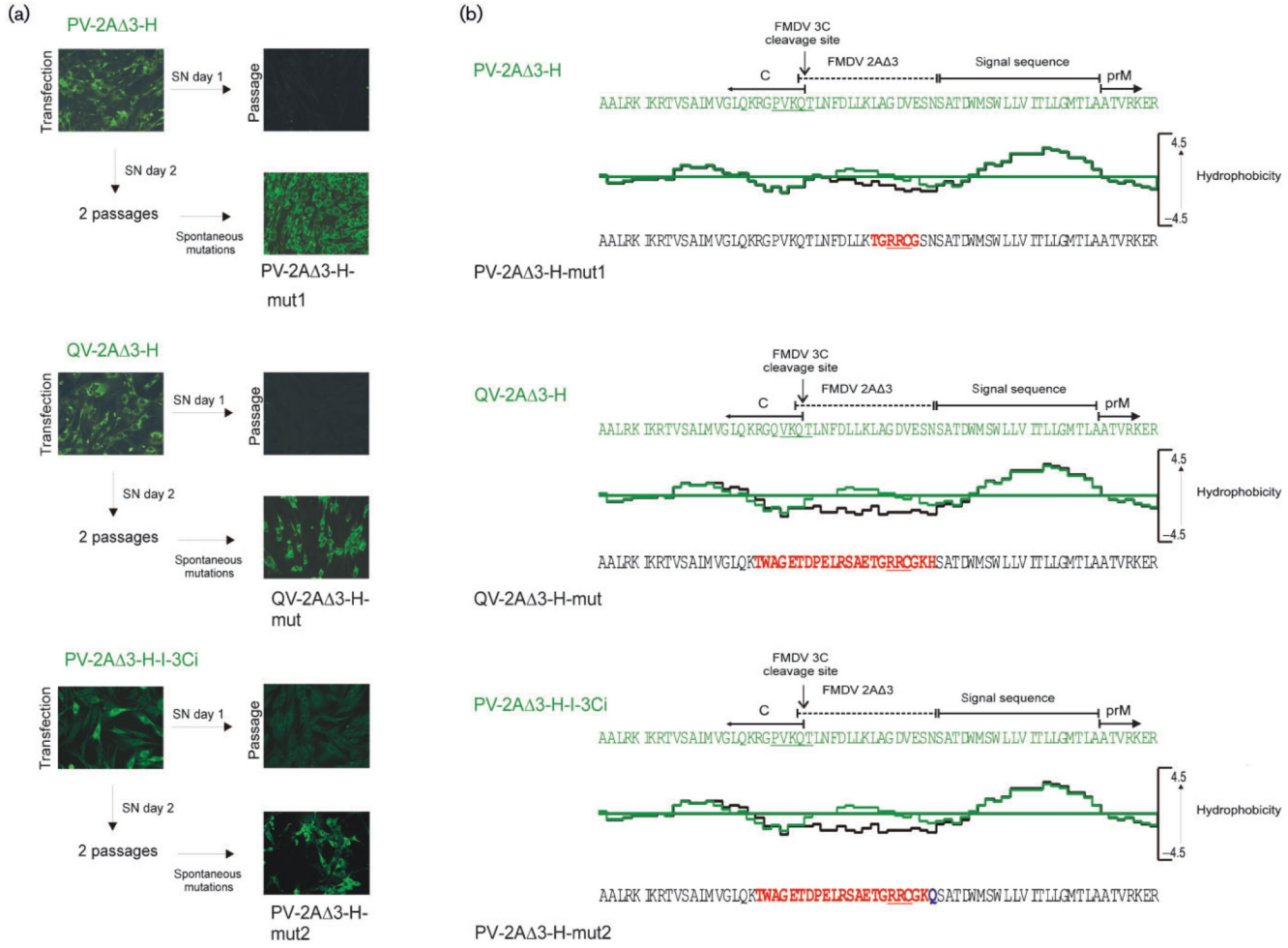

Fig. 5.

Emergence of PV-2AΔ3-H, QV-2AΔ3-H and PV-2AΔ3-H-I-3Ci second-site revertants whilst passaging without the corresponding $3C^{pro}$ or an inactive $3C^{pro}$, respectively. (a) IF analysis of protein expression and viral infectivity. BHK-21 cells were transfected with PV-2AΔ3-H, QV-2AΔ3-H and PV-2AΔ3-H-I-3Ci RNA and the viral protein expression was determined 1 day post-electroporation. Supernatants harvested 1 day post-transfection were transferred onto fresh BHK-21 cells (arrows), and the viral protein expression was detected by IF staining 1 day post-infection. Supernatants harvested 2 days post-transfection were also transferred onto fresh BHK-21 cells and further applied to two more passages on BHK-21 cells. Viral protein expression was finally detected on day 1 after the second passage by IF staining. (b) Comparison of the hydrophobicity of PV-2AΔ3-H, QV-2AΔ3-H and PV-2AΔ3-H-I-3Ci with their corresponding second-site mutants using Kyle-Doolittle algorithm (window size 11). Sequences of the C-terminal part of protein C of PV-2AΔ3-H, QV-2AΔ3-H and PV-2AΔ3-H-I-3Ci are shown in green and those of PV-2AΔ3-H-mut1, PV-2AΔ3-H-mut2 and QV-2AΔ3-H-mut in black. Acquired mutations are in red. A possible NS2B/3 cleavage site is underlined in red.

Europe PMC Funders Author Manuscripts

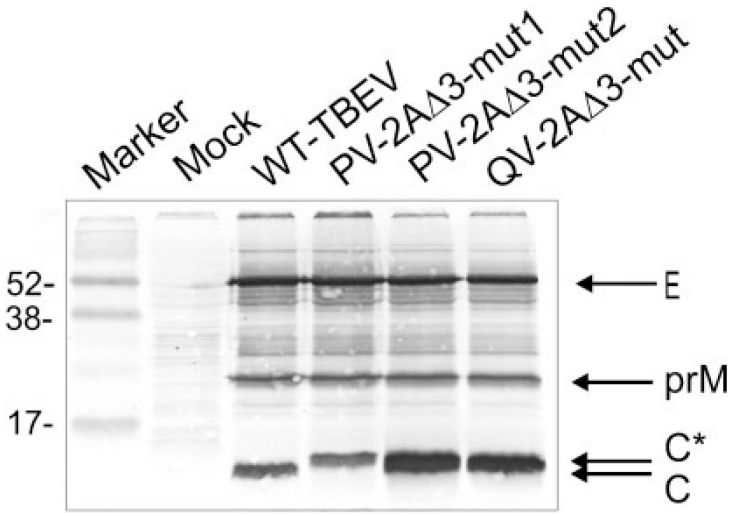

Fig. 6.

Analysis of structural-protein processing. Cells transfected with WT or mutant RNAs were lysed 48 h post-transfection, and proteins were detected by immunoblotting using a rabbit polyclonal serum against the TBEV structural proteins. Positions of proteins E, prM, C and C* as well as marker proteins in kDa are marked.

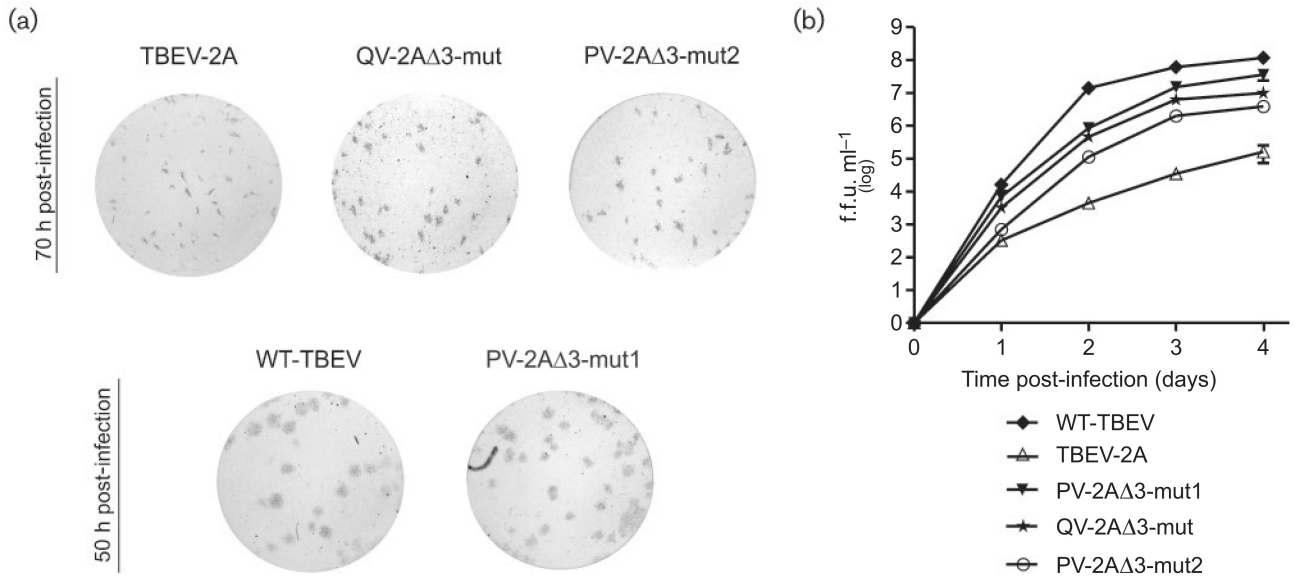

Fig. 7.

Spread and growth properties of second site revertants in BHK-21 cells. Foci morphology (a) and infectivity titres (b) were determined using a focus forming assay. BHK-21 cells were infected (m.o.i. of 0.01) and samples were taken at different times. All data points represent mean values from two independent experiments. Error bars indicate SD.

Europe PMC Funders Author Manuscripts

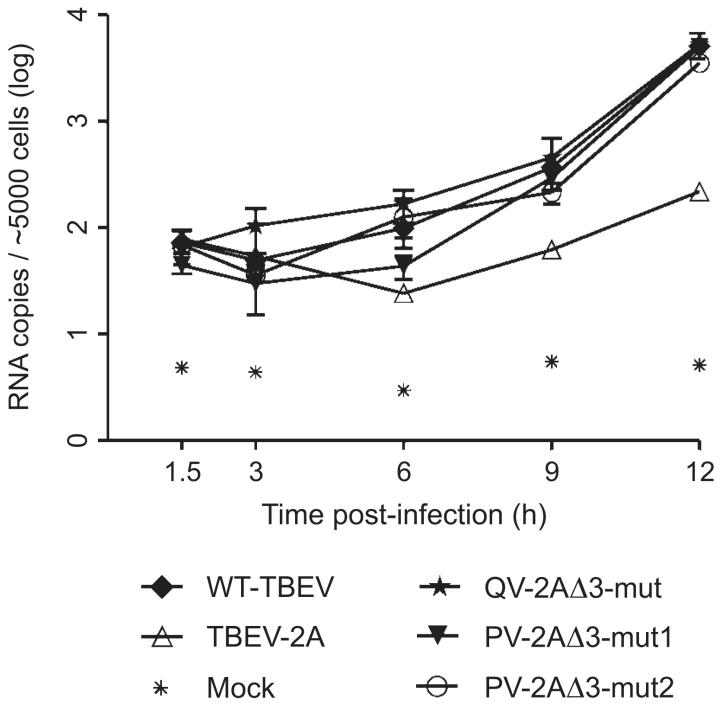

Fig. 8.

RNA replication of second site revertants, TBEV-2A and WT-TBEV after infection of BHK-21 cells. Cells were infected (m.o.i. of 1), samples were taken at different time points, and intracellular RNA levels were measured. Data points represent geometric mean values from two independent experiments. Error bars indicate standard deviations.